ISSN 1746-7659, England, UK
Journal of Information and Computing Science
Vol. 10, No. 2, 2015, *pp*. 154-160

Study of different machine learning methods in welded seam width prediction

Wang Teng [1)] *, Gao Xiangdong [2)]
1) School of Computer, South China Normal University, Guangzhou 510631, China
2) School of Electromechanical Engineering, Guangdong University of Technology, Guangzhou 510006, China
(*Received October 21, 2014, accepted February 06, 2015)*

Abstract. As an important new laser processing technique, the high-power disk laser welding has been increasingly widely used in the manufacturing area. Aiming at the strong coupling multi-variable and real-time feedback requirements of the welding process, a new method using support vector machine is proposed to predict the width of the molten pools. The performance of this model is validated by the test data. Meanwhile, analysis and comparison between the support vector machines and the BP neural network are conducted. Experiment results show that the support vector machine and the BP neural network both have a good predictive ability. However, in comparison with the BP neural network, the support vector machine is more suitable for high-power disk laser welding process.

Keywords: disk laser welding, laser-induced plume, stability, high-speed photography, different welding speeds

1. Introduction

As one of the most advanced laser welding technology, high-power disk laser welding has received a lot of attention owing to their advantages such as brilliant beam quality, high laser power, deep penetration, as well as high laser efficiency. Fields of its application ranges from the automotive and supply industries to aerospace and heavy industry.

High-power disk laser welding process is a complex process with multi-variable, which is non-linear, time-varying and vulnerable to interference. The metal vapor induced during laser welding process is related to the wavelength of the incident laser, shielding gas, welding materials and process parameters. It can provide a large number of real-time processing status information for online analysis of laser welding quality. In recent years, machine learning methods are applied to the design of welding parameters, welding performance prediction, welding process control, etc.

Machine Learning has become one of the main fields in artificial intelligence today. From the principles of statistical mechanics, a handful of algorithms have been devised to solve the regression problem. In this study, a Back Propagation (BP) algorithm and a support vector regression algorithm are studied to predict the welded seam during high-power disk laser welding. All calculations in this work were performed on a 3.0 GHz Intel(R) Pentium(R) D with 1GB RAM under windows Vista, and the calculations were carried out by using Matlab 7.0.

2. Experimental details

In this study, bead-on-plate welding at different speeds of 3, 4.5 and 6 m/min were performed on the austenitic stainless steel Type304 specimens using a high-power disk laser (TruDisk-10003) with the constant laser power of 10 kW. Table 1 lists the welding conditions. A NAC's high-speed camera system (Memrecam fx RX6) was mounted to monitor the plume and molten pool in the welding process. The optical filter was placed in front of RX6 to reduce the effect of multiple reflections between the filter and the lens. The shielding gas was argon in order to protect the molten pool from oxidation.

3. ANN models and Support vector machine

* Corresponding author. Tel.: +86-15360060605.
E-mail address of corresponding author Wang Teng: towangteng@263.net

3.1 Modeling based on BP neural network

BP networks are mainly composed of three layers of neurons: the input layer, the hidden layer and the output layer. The units of the system are connected by the weights. The input layer consists of seven neurons: the average area of metal plume P_A, the variance of metal plume area P_V, the average area of spatter S_A, the variance of spatter area S_V, the swing angle of metal plume A_S, the variance of swing angle A_V and the molten pool width of previous moment y_p, as shown in Fig. 3. Information from the input layer is then processed through the hidden layer, and the following information is computed in the output layer. The output layer includes one node: the molten pool width of previous moment y. Its unit is pixel, corresponds to 0.0386mm.

BP training algorithm is an iterative gradient algorithm, designed to minimize the mean square error between the predicted output and the actual output. The Key steps for establishment of the BP model can be summarized briefly.

Initialization: Prior to the first iteration of loop, initialize the values of the connection weights and the output threshold values of the neurons, which are random values in [-1,1].

Maintenance: Offer the input data to the neurons of the input layer. Then calculate the input and the output of neurons in the hidden layer and in the output layer. After each loop, the error between the predicted output and the actual output are propagated backward to adjust the weight in a manner mathematically guaranteed to converge.

Termination: The iteration continues until the overall error between calculated and target output is approaching to the pre-set error criteria.

3.2 Modeling based on SVR

Support vector nonlinear regression tackle regression problems by nonlinear mapping input data into high-dimensional feature spaces, wherein a linear decision surface is designed.

Assuming learning samples: $\{(x_1, y_1),...,(x_n, y_n)\} \subset R^n \times R$, support vector regression algorithm is as follows:

(1) Given the training set, $T = \{(x_1, y_1),...,(x_l, y_l)\} \subset (R^n \times R)^l$, $x_i \in R^n$, $y_i \in R, i = 1,...,l$;

(2) Select the appropriate kernel function $K(x, x')$;

(3) Select the appropriate accuracy $\varepsilon > 0$ and penalty factor $C > 0$;

(4) Introduction of Lagrange multipliers, α_i, α_i^*, construct and solve convex quadratic programming problem;

$$\min \quad \frac{1}{2}\sum_{i,j=1}^{l}((\alpha_i^* - \alpha_i)(\alpha_j^* - \alpha_j)\langle x_i \cdot x_j \rangle) + \varepsilon\sum_{i=1}^{l}(\alpha_i^* + \alpha_i) - \sum_{i=1}^{l} y_i(\alpha_i^* - \alpha_i)$$

Subject to $\sum_{i=1}^{l}(\alpha_i^* - \alpha_i) = 0 \qquad 0 \le \alpha_i^{(*)} \le C, \qquad i = 1, 2, ..., l$

giving the solution

$\bar{\alpha}^{(*)} = (\bar{\alpha}_1, \bar{\alpha}_1^*, ..., \bar{\alpha}_l, \bar{\alpha}_l^*)^{\mathrm{T}}$;

(5) Calculate $\bar{b}$: select the component of $\bar{\alpha}^{(*)}$, $\bar{\alpha}_j$ or $\bar{\alpha}_k^*$ between (0，C);

If select $\bar{\alpha}_j$ then

$$\bar{b} = y_j - \sum_{i=1}^{l}(\bar{\alpha}_i^* - \bar{\alpha}_i)K(x_i, x_j) + \varepsilon$$

If select $\bar{\alpha}_k^*$ then

$$\bar{b} = y_k - \sum_{i=1}^{l}(\bar{\alpha}_i^* - \bar{\alpha}_i)K(x_i, x_k) - \varepsilon$$

(6) Construct decision function

$$y = f(x) = \sum_{i=1}^{l}(\bar{\alpha}_i^* - \bar{\alpha}_i)K(x_i, x) + \bar{b}$$

The design of the input layer and output layer of SVR model are the same as BP model.

4. Results and discussion

We obtained 2400 laser-induced metal plume images during the experiments. The length of welding seam was 90mm, and the single image time interval was 0.5ms. If the system output sampling time interval was τ, the corresponding time interval of sampling points (the number of images included in the time interval) N was 2τ. We selected 3, 5, 10, 15 as the sampling points N, and got the corresponding sample set. 70% of the samples were selected as the training set, 30% of the samples as the test set. BP algorithm and SVR algorithm were used to train on the training set, and then use the test set to test the model. The comparison between the output of two model and the real output under N=3, 5, 10, 15 were shown in from Fig. 1 to Fig. 4. The results of BP model varied with the initial weights and thresholds. In these figures, minimum values among the outputs of BP model under the same N were selected.

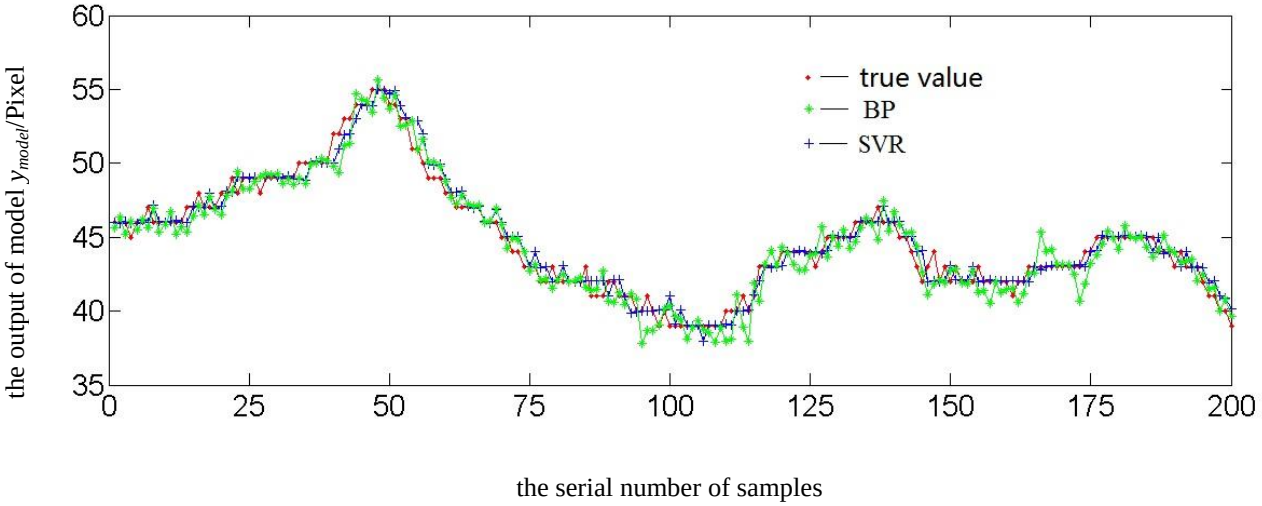

Figure 1 Testing result based on three models under N=3

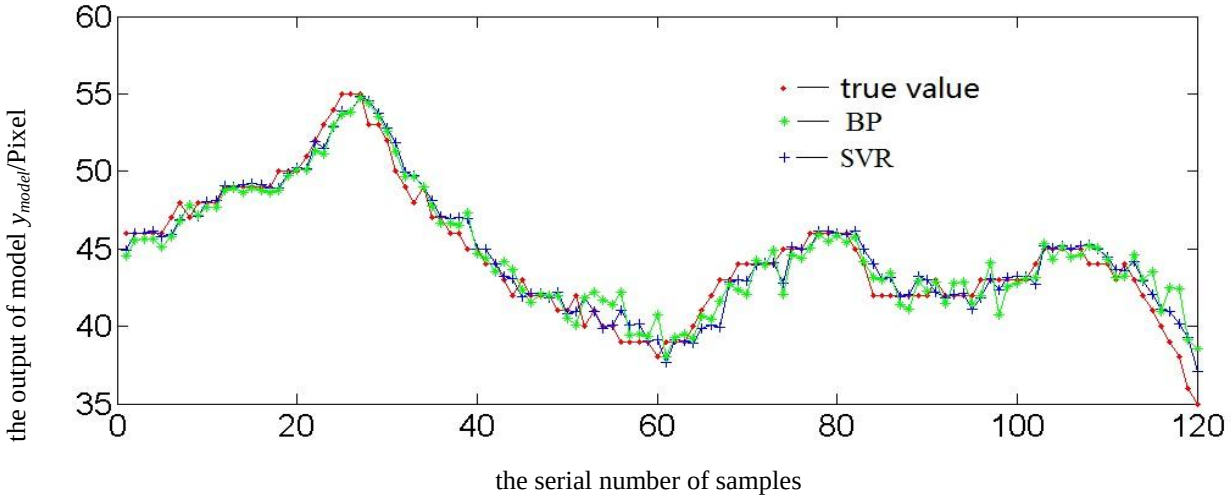

Figure 2 Testing result based on three models under N=5

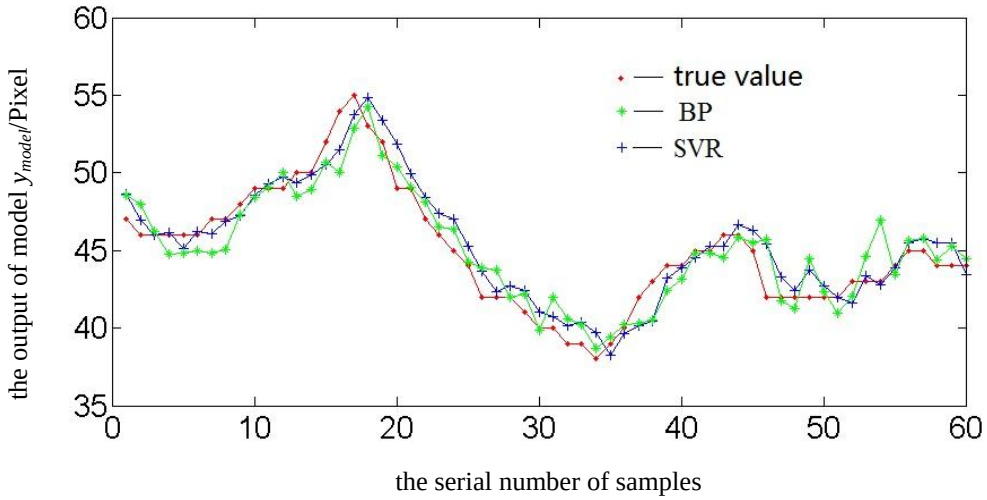

Figure 3 Testing result based on three models under *N*=10

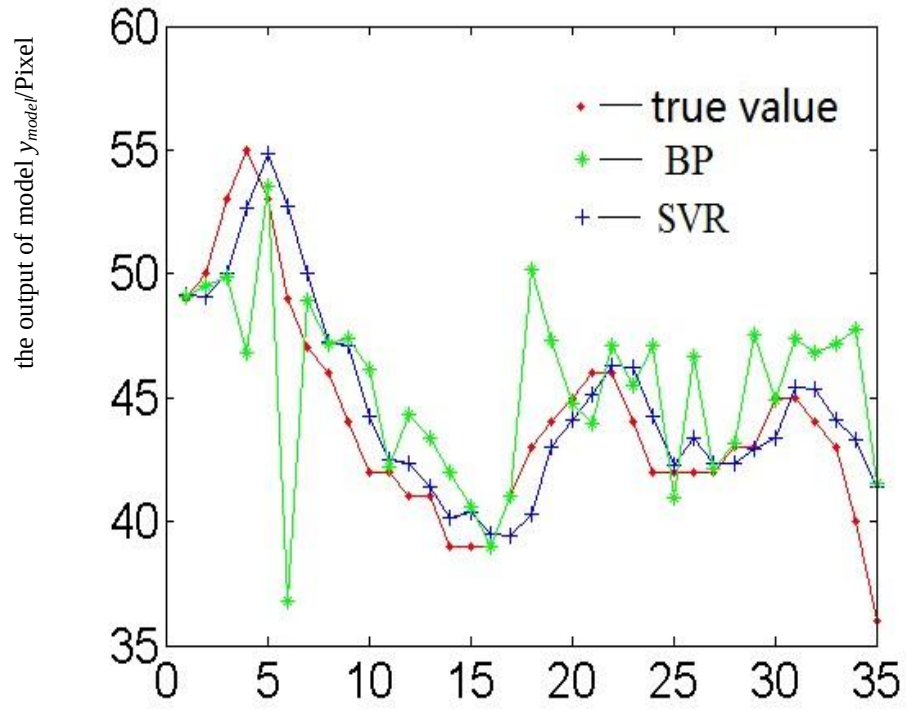

Figure 4 Testing result based on three models under *N*=15

To evaluate the training and prediction accuracy, we used Eq. 1 to calculate the mean squared errors e_{MSE} of the model.

$$e_{MSE} = \sqrt{\frac{\sum_{i=1}^{n}\left(y_{model\_output,i} - y_{real\_output,i}\right)^2}{n}} \quad (1)$$

Where y_{model_output} was the output of model, y_{real_output} was the real output, and *n* was the number of samples. Corresponding calculated results were also given in Table 1.

Table 1 Training errors and testing errors

N	BP						SVR	
	1		2		3			
	Training error e_{MSE}	Testing error e_{MSE}	Training error e_{MSE}	Testing error e_{MSE}	Training error e_{MSE}	Testing error e_{MSE}	Training error e_{MSE}	Testing error e_{MSE}
3	0.0315	0.0141	0.0292	0.0172	0.0273	0.0240	0.0189	0.0130
5	0.0257	0.0223	0.0241	0.0183	0.0240	0.0216	0.0231	0.0177
10	0.0315	0.0256	0.0310	0.0298	0.0309	0.0377	0.0365	0.0219
15	0.0316	0.0687	0.0310	0.0696	0.0306	0.0593	0.0486	0.0344

From the above table, we can see that the results of BP model were different each time under the same *N*, while the results of SVR model kept the same each time under the same *N*. The results of BP model changed according to the initial weights and thresholds. The training errors and testing errors of SVR model were monotonically increasing as *N* increased, while those of BP model had no obvious change regulation, and were related to the initial weights and thresholds. And the predictive ability of SVR model was better than BP model. When *N* is 3, the training error and the prediction error of SVR model reached the optimal value. However, the smaller *N* was, the more the number of samples were, which brought a large amount of computation. We can also see from Table 1, the training error and the testing error of SVR model has a good correlation, when the training ability was poor, the predictive ability would also be poor. But the correlation between the BP model training error and the prediction error was relatively poor. When *N* changed from 10 to 15, its training error is slightly increased, but the testing error increased sharply. This phenomenon showed that support vector machines to do non-inherent defects of linear regression generalization ability is stronger than the BP network, but also to avoid neural network - network instability, and over-reliance on the study sample, and therefore support vector machine is more suitable for the laser welding process.

Usually, when the training ability of SVR model was poor, the corresponding predictive ability would also be poor. , and in a certain extent, with the improvement of training ability the predictive ability is also improved. However, this trend approaches a limit when e_{MSE} of training set increases to 0.0310. After achieving this limit, with the improvement of the training ability the predictive ability may be decline on the contrary, which is called the over fitting phenomenon. It is because the network studies too much detail of samples and can't reflect the embedded laws of samples. We believe BP network can realize the mapped function from input to output, and mathematical theory has proved that it has the function to achieve any complex non-linear mapping. BP neural network has the ability of self-learning. It can extract the "logical" solution rules automatically through studying the examples with correct results. And BP neural network has good generalization ability.

5. Conclusion

Major conclusions obtained in this study are as follows.

(1) BP neural network and support vector machine have good training and prediction effect, and can be applied in the high-power disk laser welding process.

(2) The predictive ability of SVR model was better than BP model under the same condition.

(3) When *N* is 3, the training error and the prediction error of SVR model reached the optimal value. However, the smaller *N* was, the more the number of samples were, which brought a large amount of computation.

Acknowledgements

This work was supported by Guangdong Provincial Natural Science Foundation (2014A030310153).

6. References

[1] Kawahito Y, Matsumoto N, Mizutani M, et al. 2008, Sci. Technol. Weld. Joi., 13: 744

[2] Graham P, Stollhof J, Weiler S, et al. 2011, Proceeding of The International Society for Optical Engineering:

Frontiers in Ultrafast Optics: Biomedical, Scientific, and Industrial Applications XI, 7925: 79250T.
[3] Kouznetsov D, Bisson J F, Ueda K I. 2009, Opt. Mater., 31: 754
[4] Kim C, Kima J, Lima H, et al. 2008, J. Mater. Process. Technol., 201: 521
[5] Keskitalo M, Mäntyjärvi K. 2009, Key Eng. Mater., 410 – 411: 87
[6] Luo H, Zeng H, Hu L J, et al. 2005, J. Mater. Process. Technol., 170: 403
[7] García-Allende P B, Mirapeix J, Conde O M, et al. 2009, NDT and E Int., 42: 56
[8] Park H, Rhee S, Kim D. 2001, Meas. Sci. Technol., 12: 1318
[9] Kang H S, Suh J, Kim T H, et al. 2010, Quality monitoring of laser welding. 2010 International Conference on Control Automation and Systems, Gyeonggi-do. 2144, South Korea
[10] Seto N, Katayama S, Mizutanit M, et al. 2000, Proceeding of The International Society for Optical Engineering: High-Power Lasers Manufacturing, 3888: 61
[11] Li G H, Cai Y, Wu Y X. 2009, Opt. Lasers Eng., 47: 990
[12] Mark J, Hamprecht F A. 2009, Trans. Ind. Electron., 56: 1307
[13] Ingemar E, Per G, John P, et al. 2011, Opt. Eng., 49: 100503
[14] Wang T, Gao X D, Katayama S , et al. 2012, Plasma Sci. Technol., 14: 245
[15] Tseng D C, Chang C H. 1992, Color segmentation using perceptual attributes, in the Proc. of the 11th Int. Conf. on Pattern Recognition (Hague, the Netherlands, 1992), IAPR, New York, Vol. III, 228, IEEE Computer Society Press, Washington